Instability threshold versus switching threshold in spin-transfer-induced magnetization switching

T. Devolder,* P. Crozat, and C. Chappert
Institut d'Electronique Fondamentale, UMR 8622 CNRS, Université Paris Sud, Bâtiment 220, 91405 Orsay, France

J. Miltat
Laboratoire de Physique des Solides, UMR 8502 CNRS, Université Paris Sud, Bâtiment 510, 91405 Orsay, France

A. Tulapurkar and Y. Suzuki
Nanoelectronics Research Institute, National Institute of Advanced Industrial Science and Technology, Tsukuba 305-8568, Japan

K. Yagami
MSNC, Semiconductor Technology Development Group, SONY Corp., Atsugi, Kanagawa, Japan
(Received 6 October 2004; published 3 May 2005)

We study the magnetization dynamics induced by spin-angular momentum transfer in pillar-shaped CoFe/Cu/CoFe spin valves in zero-applied magnetic field. The voltage noise generated by the spin flow is used to identify the microwave magnetic excitations. In the bistable region of resistance (R) versus current (I) traces, a resonant magnetic excitation at 8 GHz is pumped above a first threshold identified as the instability current. Higher currents are required to induce switching. Between the instability current and the switching current, a reversible rounding of the $R(I)$ hysteresis loop is observed. Numerical modeling indicates that it arises from a current-induced dynamic instability of the magnetization: When a state with collinear magnetizations is driven unstable, the magnetization of the thinnest ferromagnetic layer undergoes a sustained precession along a large orbit. The simulated precession orbit is stationary at 0 K and randomly perturbed at 300 K, and its main characters are in quantitative agreement with the experiment.

DOI: 10.1103/PhysRevB.71.184401 PACS number(s): 75.60.Ej, 72.25.Pn, 75.70.−i

In a seminal paper,[1] John Slonczewski predicted in 1996 that a large electrical current could be used to toggle the magnetization of the thinnest magnetic layer of a giant magnetoresistance (GMR) junction in the current perpendicular-to-plane (CPP) geometry. The driving force is the transfer of spin-angular momentum from the conduction electrons to the magnetization; the transverse component of the incoming spin flow is absorbed near the interface as a result of spin filtering, differential spin reflection, and incoherent spin precession.[2]

Owing to its interest for magnetic random access memories (MRAM), Slonczewski's paper triggered several experimental implementations of the current-induced hysteretic switching that confirmed the prediction.[3–5] Yet the dual consequence of the spin-angular momentum transfer effect is that the associated torque acting on the magnetization should resonantly emit spin waves[6] and drive steady-state magnetization precession.[7,8] Experimentalists observing anomalies in the I-V characteristics interpreted[9] them as an indirect evidence for this stimulated emission of spin waves. These excitations were later observed directly, mostly in a frustrated situation where large applied fields favoring the parallel (P) magnetizations compete with large negative currents favoring the antiparallel (AP) magnetizations.[10,11] In this frustrated regime, large precessions are excited, with potential applications to microwave oscillators that could be tunable through the combination of a large current and a high magnetic field. In contrast, little work has been dedicated to the case when the action of the current is not counterbalanced by a static applied field. The corresponding zero-field magnetic excitations deserve to be studied. Indeed, they are those pumped in a spin-transfer switching event, and they may impact the switching speed.[12]

Our present paper focuses on the magnetization excitations in this subswitching current regime under *zero*-applied field. By measuring the microwave GMR noise in the bistable part of the current-induced hysteresis, we observe high-amplitude magnetic excitations at 8 GHz and correlate them with remanence measurements relying on dc GMR. We conclude that the magnetization does not at all stay at rest below the switching threshold. Indeed, when sweeping the current above a first threshold, a dynamic instability grows and the magnetization starts to precess along a quasistationary orbit, as corroborated by finite temperature simulations in the macrospin approximation. At higher currents switching occurs. This two-step reversal scenario may have implications for the spin-transfer switching speed.

The samples are pseudo-spin valves $Co_{75}Fe_{25}(t=2.5\ \text{nm})/Cu(6\ \text{nm})/Co_{75}Fe_{25}(40\ \text{nm})$ patterned in a pillar geometry [Fig. 1(a)] using the standard steps of electron-beam lithography and liftoff. The top layer is patterned into an ellipse of size $2a\times 2b=173\times 80\ \text{nm}^2$, while the bottom layer extends all over the metallic parts of the device [Fig. 1(b)]. The spontaneous magnetizations of the thin and thick magnetic layers were measured prior to patterning. They are 1.5×10^6 and 1.7×10^6 A/m, respectively. The patterned thin layers have coercivities from 15 to 40 mT and the thick layer has a coercivity of 2 mT. The other magnetic properties were quite similar from sample to sample. We define x and y as the easy and hard axes of the (top) thin layer, respectively. The pillar is contacted in the CPP geometry to measure its GMR. A current of 1 mA corresponds to

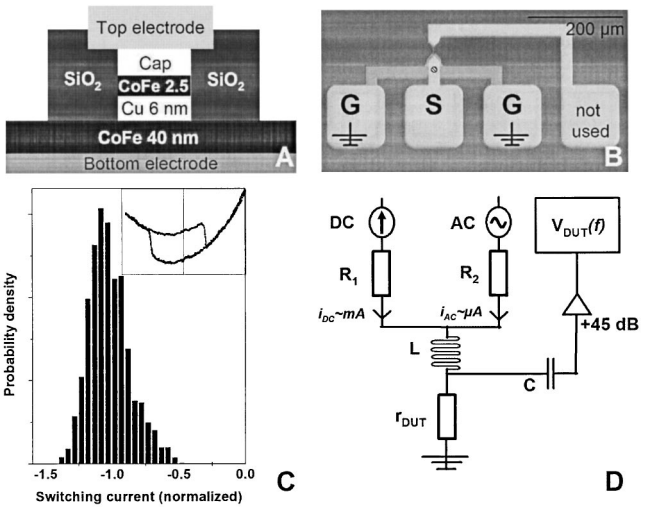

FIG. 1. (a) Cross section of the device under test. Lateral size is 80×173 nm^2. (b) Optical micrograph of the high bandwidth accesses to the device (central dot). (c) Histogram of the distribution of the AP$\rightarrow$P switching currents (from 5040 switching events). Inset: R vs I_{dc} hysteresis loop. (d) Sketch of the measurement setup.

a current density of 9.2×10^6 A/cm^2. The bottom contact is short-circuited to the ground (G), while the top electrode (signal electrode *S*) is contacted to microwave coplanar pads. The overall resistance is about $R\approx7\ \Omega$ while the magnetoresistance variation is $R_{AP}-R_P=130$ mΩ. The overall size of the layout fits into a $300\times600\ \mu$m^2 area. Taking into account the substrate (Si) relative permittivity $\varepsilon_r=11.7$, the circuit can be considered as a localized impedance up to 30 GHz. Scattering matrix microwave measurements indicate that the overall circuit shunt capacitance is $C_{shunt}\approx10$ pF and that the device electrical bandwidth is related to the RC_{shunt} product (13 GHz).

The setup aims at measuring simultaneously the slow time dependence of the resistance $R(t)$ and its frequency dependent noise $R_{noise}(\omega)$ in the band 100 MHz to 18 GHz. For that purpose, the device coplanar pads are contacted with coaxial waveguides of bandwidth 40 GHz to the instruments. They allow for the simultaneous application and measurement of three electrical currents I_{DC}, I_{AC}, and I_{RF} in separate frequency domains [Fig. 1(d)]. The triangular ramp current ($I_{DC}\sim$ mA, $f\leqslant3$ Hz) induces the quasistatic switching of the magnetization of the top thin layer using the spin-transfer effect [Fig. 1(c), inset]. A small modulation current ($I_{AC}=36\ \mu$A rms, $f=100$ kHz) is superimposed to allow for the measurement of the resistance $R(t)$ with a lock-in amplifier. These low-frequency currents are routed in the device through the dc (inductive) port of a bias tee.

Any microwave fluctuation of the magnetization directions of the magnetic layers induces a microwave variation of the CPP resistance, hence a variation of the voltage V_{RF} across the pillar device. The RF (capacitive) port of the bias tee transmits this V_{RF} to cascaded, low noise (3 dB noise factor) broad band (100 MHz–18 GHz) amplifiers that feed the input of a 26-GHz spectrum analyzer [Fig. 1(d)] with 2-MHz resolution bandwidth. The actual noise power emitted by the pillar device is calculated after correction of the impedance mismatches. No external magnetic field is applied[13] and the experiments are performed at room temperature.

Note that in these kind of noise analysis experiments, one usually applies[14] a hard axis field (along y) to make the two layers' magnetizations noncollinear and therefore gain a *linear* sensitivity to $m_y(t)$. Unless doing so, the signal is usually quadratic in $m_y(t)$. Although we apply no magnetic field, there may still be a finite angle between the layers' magnetizations because the anisotropy axes have no reason to be strictly collinear; the anisotropy of the free layer comes from its shape, whereas that of the thick layer comes from its crystalline structure. We write θ the spatial average of this noncolinearity angle, and $\Delta\theta$ its time-varying part. The high-frequency voltage V_{RF} across the pillar device then scales with $m_y(t)$, and accounts for the frequency of the magnetic excitations with a sensitivity related to the power $P_{RF}=I_{DC}{}^2\Delta R\Delta\theta\sin\theta$.

In spin-transfer switching experiments, sweeping back and forth the CPP current switches back and forth the magnetization of the thin layer [Fig. 2(a)]. No stable state of resistance intermediate between R_P and R_{AP} was ever observed in the present experiments. For both states, the resistance does not change in a given interval from $I_{DC}=0$ to $I_{DC}{}^{rounding}$. The resistance then starts to change smoothly, as illustrated by the dotted line slope in Fig. 2(a). Above a greater current, hereafter referred to as the switching current $I_{DC}{}^{P\rightarrow AP}$ or $I_{DC}{}^{AP\rightarrow P}$, the resistance changes very abruptly. $I_{DC}{}^{rounding}$ is 0.9 mA for the AP to P transition and -1.4 mA for the P to AP transition [Fig. 2(a)]. Such a rounding of the loop between $I_{DC}{}^{rounding}<I<I_{DC}{}^{switch}$, i.e., just before the switching, has already been observed by several authors and was recently attributed to the excitation of dynamical states.[15] For both polarities, the switching current varies from one measurement to another. On a given sample, the standard deviation is 14%. The histogram of the $I_{DC}{}^{AP\rightarrow P}$ transition [Fig. 1(c)] has a substantial skew towards the small currents. Conversely, the high-current part of the distribution is narrower; a cutoff current does exist for which switching is always obtained. The average values of the switching currents are $I_{DC}{}^{P\rightarrow AP}=-2.2$ mA (i.e., 2×10^7 A/cm^2) for the parallel (P) to antiparallel (AP) transition. The AP to P requires less current, typically $I_{DC}{}^{AP\rightarrow P}=1.7$ mA (i.e., 1.6×10^7 A/cm^2).

In order to understand the origin of the loop rounding, we measured the CPP resistance noise spectrum [Fig. 2(b)] during the $R(I)$ hysteresis loop, and more specifically near the P to AP transition. The noise spectra in the remanent P and AP states were white and near the noise floor of the setup. No specific feature could be detected in the spectra. This holds true until the current I_{DC} is raised above $I_{DC}{}^{rounding}$, where a sharp peak grows at 8.3 GHz, with a full width at half maximum (FWHM) $\Delta\omega=0.2$ GHz [Figure 2(b)]. Precession of the magnetization is thus preferentially excited at the above-mentioned frequency. As we approach $I_{P\rightarrow AP}{}^{switch}$, the resonance peak grows only marginally. A substantial lower frequency shoulder, however, appears, which deviates away from the main peak with growing current [Figure 2(b)]. At $I_{DC}=-2.25$ mA, the magnetic junction emits a total noise

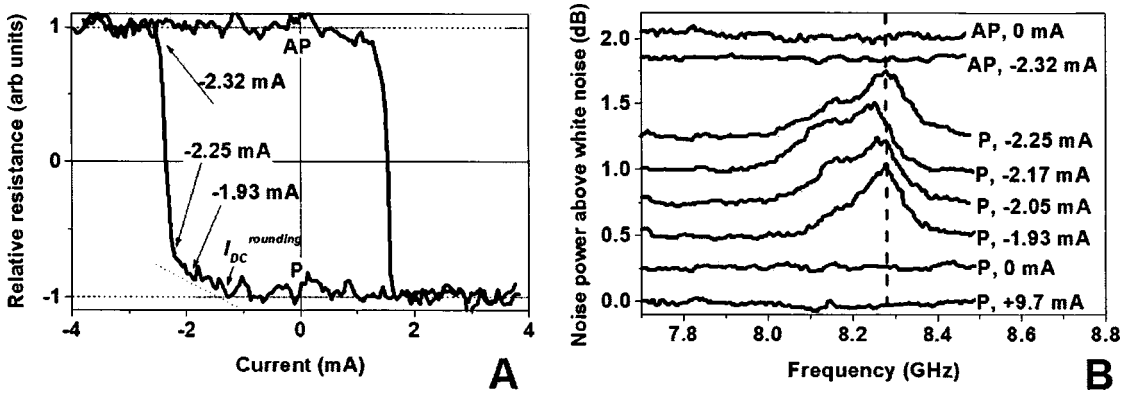

FIG. 2. (a) Quasistatic resistance vs current hysteresis loop. A global curvature was cancelled. The dotted line near the P→AP transition recalls the presence of a systematic reversible part of the loop where there is a faint but unequivocal finite slope. (b): Noise power above white noise around 8.2 GHz in various magnetic configurations: at zero current, at high current in the P state, and before and after the P→AP transition. The curves were vertically offset for clarity. The labeled dc current are defined with an uncertainty equal to the ac modulation, i.e., ±0.05 mA.

power of 11 pW. This microwave resonant excitation disappears immediately when the sample switches to the AP configuration. No other feature in the frequency spectrum is observed when increasing the current further. Also, no feature is observed in high positive current stabilizing the P configuration [Fig. 2(b)].

Before entering a more detailed analysis, it ought to be emphasized that in addition to the rounding, a positive curvature is present in the $R(I)$ curves. This fact is often simply attributed to Joule heating. However the P and AP branches of the loop display different curvatures; the curvature in the P branch being significantly higher [see inset in Fig. 1(c)]. These nonthermal parabolic contributions that differ in the P and AP branches arise from the ampere field H_{amp} generated by I_{DC}. Indeed, H_{amp} has azimuthal symmetry and reaches up to about 3 mT. Since this is much smaller than the shape anisotropy field of the thin layer, the latter mainly remains a macrospin aligned with its easy axis. In contrast, the ampere field deforms the micromagnetic state of the (much softer) thick layer into a *C*-like state: The central part of the thick layer ($|x| \ll a$) is unaffected while below the tips ($x \approx \pm a$) of the ellipse, the remanence is reduced ($m_x < 1$) and a finite odd transverse magnetization appears $m_y\ (x=a) = -m_y(x=-a)$, which scales with H_{amp}. The resistance of such a micromagnetic configuration is equivalent to that arising from two macrospins misaligned by an angle θ_0 with a typical value of $m_y(x=a)/2$.

In the P state, this magnetization bending due to the ampere field increases the CPP resistance away from R_P with a sensitivity scaling with $\cos\theta_0$, i.e., scaling with $H_{amp}{}^2$, hence with $I_{DC}{}^2$. As a result, the ampere field *increases* the CPP resistance in the P branch *above* R_P, *with a positive parabolic curvature versus* I_{DC}. The situation is opposite in the AP state: The ampere field closes the angle between the magnetizations of the thick and thin layers leading to a *decrease* of the resistance below R_{AP} *with a negative parabolic curvature versus* I_{DC}. Comparing the loop curvatures in the P and AP branches [Fig. 1(c), inset], we derived both the Joule effect and an estimation of θ_0 vs I_{DC}. The noncollinearity angles θ_0 are of the order of $\theta_0 = 20°$ for currents close to $I_{DC}{}^{rounding}$. The present results may now be summarized as follows: (i) Confirming previous reports,[3] the switching current is probabilistic. The probability distribution has a significant low current tail [Figure 1(c)]. (ii) Most single-trace hysteresis loops [Fig. 2(a)] exhibit a slope between $|I_{DC}{}^{rounding}| < |I| < |I_{DC}{}^{switch}|$ i.e., before switching. This slope correlates with the onset of a magnetization precession centered around 8.3 GHz, with a linewidth of $\Delta f = 200$ MHz at $I_{DC}{}^{rounding}$. A shoulder near 8.1 GHz separates from the main peak when approaching $I_{DC}{}^{switch}$. The resonance disappears when the system switches.

The transfer of spins is usually modeled[7,16] by incorporating a "spin torque" in the Landau-Lifshitz-Gilbert (LLG) equation describing the time evolution of the reduced magnetization $\mathbf{m}(t)$ of the thin layer. This torque is $Gj\mathbf{m}\times(\mathbf{m}\times\mathbf{u})$ where $\mathbf{u}$ is the direction of the itinerant spin orientation. The torque G per current density j scales with the spin polarization and inversely with the thin layer thickness. Note that the G's are different in P and AP configurations.[2] Analytical descriptions of the switching current were so far restricted to the macrospin approximation. For instance, in the model of Katine *et al.*[17] and its extensions,[5] the switching current is calculated by assuming that the stability of the P state together with the instability of the AP state are *sufficient* conditions to trigger switching from the AP to P states. In the small amplitude limit, the magnetization evolves as $m_y \sim e^{-kt}\cos(\omega t)$; the switching was thus assumed[5] to occur for a current density corresponding to $k=0$, which reads

$$j^{instability} = \frac{\alpha\gamma_0}{2G}(2H_k + M_S), \tag{1}$$

while the elementary excitations around $j^{intability}$ have frequencies $\omega/2\pi$ equal to

$$\omega = \gamma_0\sqrt{M_S\left(H_k - \frac{\alpha G j}{\gamma_0}\right)} \tag{2}$$

Note that reasonable parameters lead typically to $\alpha G j/\gamma_0 H_k < 0.1$, so that the spin-transfer effect is only a minor correction to the zero-field ferromagnetic resonance

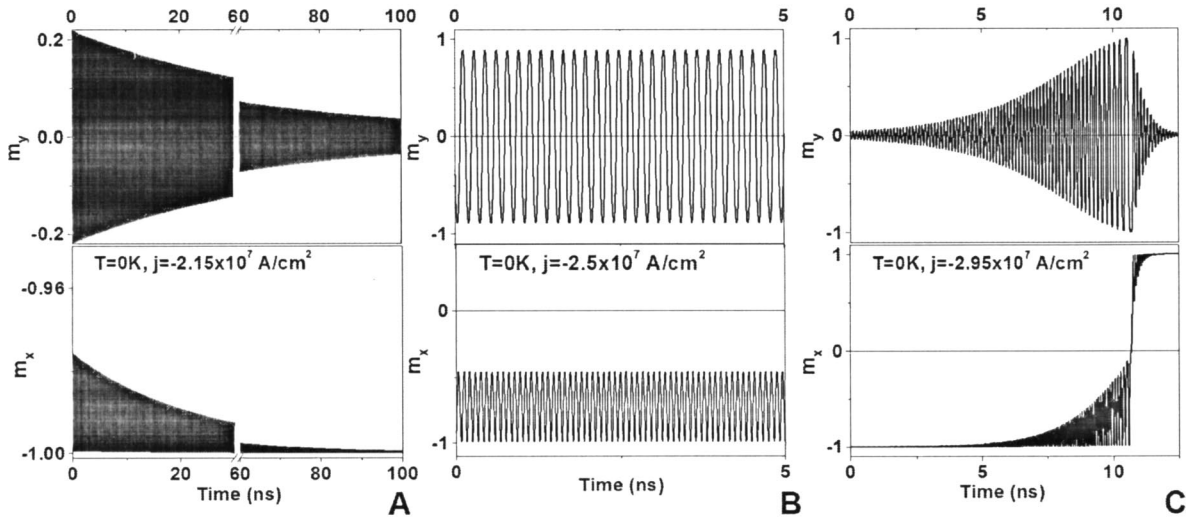

FIG. 3. Calculated macrospin trajectories $m_y(t)$ and $m_x(t)$ at $T=0$ K for various applied currents and an initial magnetization off the easy axis. (a) $I_{DC}=-2.15\times10^7$ A/cm^2: slightly damped precession in the regime $|I_{DC}|<|I_{DC}^{instability}|\approx2.25\times10^7$ A/cm^2. (b) $I_{DC}=-2.5\times10^7$ A/cm^2: settled steady-state precession. The current is in the interval $|I_{DC}^{instability}<|I_{DC}|<|I_{DC}^{switch}|\approx2.7\times10^7$ A/cm^2. (c) $I_{DC}=-2.95\times10^7$ A/cm^2: gradually pumped precession leading to a switching event.

(FMR) frequency of the free layer. The anisotropy field can thus be obtained by Eq. (2) which provides $\mu_0 H_k=45$ mT. In our experimental data, this value is in agreement with $\mu_0 H_k=48$ mT obtained by numerically calculating the demagnetization tensor of the patterned thin layer. Despite such a nice agreement, analytical theories[17,5] cannot account for two major experimental facts;[18]

(i) The rounding of the hysteresis loop and the existence of narrow linewidth excitations between $|I_{DC}^{rounding}|<|I|<|I_{DC}^{switch}|$ are clear indications of the existence of stationary states that are neither P nor AP. For these states, the magnetizations of the thick and thin layer are neither static nor collinear; the small angle approximation leading to the analytical expression of the switching current [Eq. (1)] thus becomes questionable.

(ii) Analytical theories cannot account for the resonance linewidth. Indeed, owing to the approximation used in, e.g., Ref. 5, the energy dissipated by damping and the energy provided by the spin flow compensate exactly (i.e., $k=0$) over one precession period when Eq. (1) applies. Consequently, the resonance of $m_y(t)$ at $I=I^{instability}$ should have an infinitely narrow linewidth $\Delta\omega=0$. We observe a trend in contradiction to this predicted collapse of $\Delta\omega$. We are thus led to the conclusion that models assuming that the stability and instability criteria of the P and AP states is a *sufficient* condition for switching cannot account for the magnetization dynamics in the range $|I_{DC}^{rounding}|<|I|<|I_{DC}^{switch}|$.

In order to better describe the experimental behavior in that current interval, we have solved numerically the modified LLG equation, assuming a macrospin approximation for the thin layer and a fixed thick layer magnetization, following the methods initiated by Sun *et al.*[7] or Miltat *et al.*[16] Owing to the macrospin approximation, the exact distribution of current paths does not matter. In the displayed calculations, we ramp a negative, uniform current density starting from the P state in zero current. Qualitatively similar results would be obtained for the AP to P transition (not shown). M_S and H_k are equal to their respective experimental values, while G assumes a constant electron-spin polarization of 30% near the P state and the damping parameter has been chosen equal to 0.006. The calculated trajectories of the magnetization vector at $T=0$ K are displayed in Fig. 3. In contrast to the analytical theories and as already noted in Ref. 7, the calculations identify three unequivocal regimes at 0 K: (a) the damping-dominated regime, (b) the stationary precession regime, and (c) the switching regime. These regimes still qualitatively exist at 300 K, but the random nature of thermal activation blurs the transitions between regimes. Regime *A* occurs below $I_{instability}$. The P state is unperturbed by the spin flow. Any finite fluctuation is damped down [Fig. 3(a)]. The precession frequency follows Eq. (2). In regime *B*, i.e., above $I_{instability}$, the P state is driven unstable and any finite fluctuation is amplified until the magnetization precesses along a stationary orbit around the P position [Figure 3(b)]. The in-plane fanning angle $\Delta\theta$ of this excitation grows with increasing current (not shown). Meanwhile, the excitation frequency decreases significantly above $I^{instability}$ (≈-1 GHz per 10^6 A/cm), in opposition to Eq. (2). The switching regime *C* finally occurs when the current exceeds another threshold I_{switch}. The fanning angle $\Delta\theta$ reaches 180° and the orbit extends beyond the hard axis. The magnetization reverses and is then quickly damped around the AP state [Fig. 3(c)] and a full remanence is quickly reached. Note that at zero temperature, the trajectories when $|I_{DC}^{instability}|<|I|<|I_{DC}^{switch}|$ [i.e., regime *B*: stationary precession] are perfectly periodic after the initial settling time [Figure 3(b)]. The corresponding power density spectra are Dirac peaks (not shown). Note that this holds because of the assumed macrospin approximation and the zero temperature.[19]

Conversely, at 300 K, the magnetization trajectories are affected by the random thermal fluctuations [Fig. 4(a)]. The

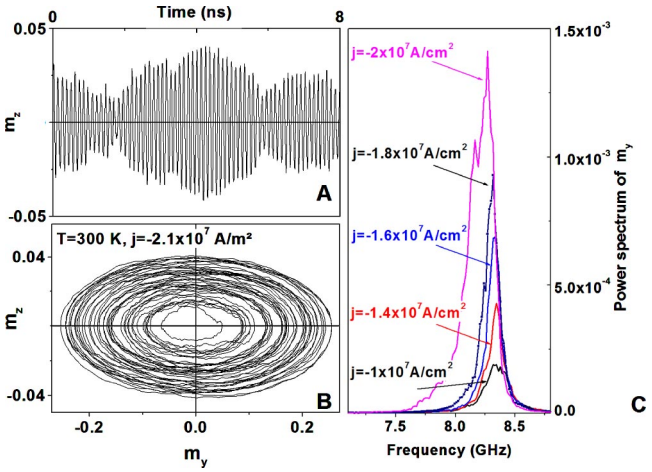

FIG. 4. (Color online) Calculated macrospin trajectories at $T=300$ K for an initial magnetization slightly off the easy axis and for an applied current slightly below the switching threshold. (a) $I_{DC}=-2.1\times10^7$ A/cm^2 and $T=300$ K; m_z component vs time. (b). $I_{DC}=-2.1\times10^7$ A/cm^2 and $T=300$ K; precession amplitude visualized as the out-of-plane component m_z vs the hard axis component m_y of the magnetization during 5 ns. (c). Calculated power density spectra of $m_y(t)$ at $T=300$ K in the quasistationary regime for increasing CPP spin flow in the interval $|I_{DC}{}^{instability}|<|I_{DC}|<|I_{DC}{}^{switch}|\approx2.3\times10^7$ A/cm^2.

precession amplitude [Fig. 4(b)] and period fluctuate with time, leading to 200–400 MHz linewidths in the power density spectra, in agreement with the experiment [Fig. 4(c)]. Another important difference induced by the large temperature is that the excitation frequency does not vary much with current, a rather unique feature that also is in quantitative agreement with the experiments. For current densities above -2.3×10^7 A/cm^2, the precession amplitude fluctuates so much that a switching event occurs after a random delay, typically some microseconds.

The calculated dynamics accounts well for our experimental data at room temperature, except that the calculation predicts a much more gradual increase of the resonance amplitude with the current. At low current [damping-dominated regime *A*] the unperturbed P state correlates with the full remanence measured below $I_{rounding}$ [Fig. 2(a)] and the absence of any significant microwave magnetic excitation [Fig. 2(b)]. At higher current, i.e., $|I_{DC}{}^{instability}|<|I|<|I_{DC}{}^{switch}|$, the calculated sustained precession [Fig. 4(a)] correlates with the experimental resonance at 8.3 GHz observed when $|I_{DC}{}^{rounding}|<|I|<|I_{DC}{}^{switch}|$. A consequence is that we can reliably identify the calculated $I_{DC}{}^{instability}$ and the measured $I_{DC}{}^{rounding}$. An additional argument in favor of this identification is the fact that the precession amplitude is so large that the calculated time average of m_x is smaller than 1, which correlates with the experimental increase of resistance away from R_P (corresponding to $\theta_0=\Delta\theta=0$) in the rounding of the quasistatic loop when $|I_{DC}{}^{rounding}|<|I|<|I_{DC}{}^{switch}|$. The measured and calculated small skew of the resonance line are a classical consequence of the growing precession amplitude,[20] while the resonance shoulder may arise from nonmacrospin or ampere field contributions that are indeed neglected in our model. The ampere field is zero in the central part of the sample and should not shift the frequency of the main mode, as observed in experiments [dotted vertical line in Fig. 2(b)]. In contrast, the excitation modes near $x=\pm a$ feel a different spin torque because $\theta_0\neq0$ in those regions. Similarly precession modes near $y=\pm b$ are subject to an increased or decreased restoring torque due to the ampere field.

In conclusion, we have studied the magnetization dynamics in the presence of spin angular momentum transfer in pillar-shaped pseudo-spin valves CoFe(2.5 nm)/Cu/CoFe(40 nm). The magnetoresistance noise excited by the spin flow was correlated to the dc magnetoresistance. In the hysteretic part of resistance versus current traces, the resistance departs reversibly from the resistance at remanence when approaching the irreversible switching threshold. This dc loop rounding correlates with the growth of a resonant, high amplitude excitation of the free layer's magnetization at 8.3 GHz, i.e., a frequency close to the zero-field ferromagnetic resonance. Numerical modeling based on a generalized Landau-Lifshitz equation indicates that the rounding and the microwave resonance both result from a current-induced dynamic instability of the magnetization that occurs below the switching current. When a state with collinear magnetizations (either parallel or antiparallel) is driven unstable, the magnetization does not reverse at first but rather precesses along a large orbit which is stationary only at zero temperature.

This work was supported by the European Communities Human Potential program under Contract No. HRPN-CT-2002-00318 ULTRASWITCH.

*Author to whom correspondence should be addressed. FAX: (33) 169157841. Email address: thibaut.devolder@ief.u-psud.fr

[1] J. Slonczewski, J. Magn. Magn. Mater. **159**, 1 (1996).
[2] M. D. Stiles and A. Zangwill, Phys. Rev. B **66**, 014407 (2002).
[3] E. B. Myers, F. J. Albert, J. C. Sankey, E. Bonet, R. A. Buhrman, D. C. Ralph, Phys. Rev. Lett. **89**, 196801 (2002).
[4] F. J. Albert, N. C. Emley, E. B. Myers, D. C. Ralph, R. A. Buhrman, Phys. Rev. Lett. **89**, 226802 (2002).
[5] J. Grollier, V. Cros, H. Jaffrès, A. Hamzic, J. M. George, G. Faini, J. Ben Youssef, H. Le Gall, and A. Fert, Phys. Rev. B **67**, 174402 (2003).
[6] L. Berger, Phys. Rev. B **54**, 9353 (1996).
[7] J. Z. Sun, Phys. Rev. B **62**, 570 (2000).
[8] Z. Li and S. Zhang, Phys. Rev. B **68**, 024404 (2003).
[9] M. Tsoi *et al.*, Phys. Rev. Lett. **80**, 4281 (1998).
[10] S. I. Kiselev, J. C. Sankey, I. N. Krivorotov, N. C. Emley, R. J. Schoelkopf, R. A. Buhrman, and D. C. Ralph, Nature (London) **425**, 380 (2003).
[11] W. H. Rippard, M. R. Pufall, S. Kaka, S. E. Russek, and T. J. Silva, Phys. Rev. Lett. **92**, 027201 (2004).

[12] A. A. Tulapurkar, T. Devolder, K. Yagami, P. Crozat, C. Chappert, A. Fukushima, Y. Suzuki, Appl. Phys. Lett. **85**, 5358 (2004).

[13] When electrical current flows in the device, the magnetic fields created by the ground lines cancel each other at the device's location. The magnetic field generated by the signal line do not exceed 50 μT.

[14] S. E. Russek, R. D. McMichael, M. J. Donahue, in *Spin Dynamics in Confined Magnetic Structures*, edited by B. Hillebrands and K. Ounadjela (Springer, Berlin, 2003), Vol. II.

[15] I. N. Krivorotov, N. C. Emley, A. G. F. Garcia, J. C. Sankey, S. I. Kiselev, D. C. Ralph, and R. A. Buhrman, Phys. Rev. Lett. **93**, 166603 (2004).

[16] J. Miltat, G. Albuquerque, A. Thiaville, and C. Vouille, J. Appl. Phys. **89**, 6882 (2001).

[17] J. A. Katine, F. J. Albert, R. A. Buhrman, E. B. Myers, and D. C. Ralph, Phys. Rev. Lett. **84**, 3149 (2000).

[18] While correcting this manuscript, the authors received a private communication from T. Valet, describing an analytical theory in good agreement with their experimental findings.

[19] A full micromagnetic calculation (not shown) takes into account the nonuniformity of the demagnetizing field that results from the nonellipsoidal sample shape. This nonuniformity is sufficient to engender a resonance finite linewidth even at zero temperature.

[20] T. Devolder and C. Chappert, Solid State Commun. **129**, 97 (2004). It is well known from high-power FMR experiments that when the fanning angle $\Delta\theta$ enlarges, the time average of the restoring torque $H_k\langle m_x(t)\rangle$ decreases, which leads to a decrease of the resonance frequency.